

SIMULATION STUDIES OF CONTRACTING SKELETAL MUSCLES DURING MECHANICAL STRETCH*

A. CROWE,† H. VAN ATTEVELDT and H. GROOTHEDDE

Department of Medical and Physiological Physics, Experimental Physics Laboratory,
State University of Utrecht, Princetonplein 5, Postbus 80.000, 3508 TA Utrecht,
The Netherlands

Abstract – A form of the sliding filament model is presented to simulate the experimentally observed phenomena when a contracting muscle is subjected to mechanical stretches. It is assumed that the cross bridges can be extended to provide extra tension and that they can be broken if a critical limit of extension is exceeded. Passive components, including non-linear parallel elasticity are incorporated in the model. Such effects as short-range stiffness, the slip effect and excess tension after mechanical stretch can be simulated. The simulations are compared with our own experimental tests on frog sartorius muscle and with previously reported results from other muscle preparations.

Key words – Mechanical properties, skeletal muscle, isometric tension, rap and bold studies.

INTRODUCTION

In the preceding paper (Van Atteveldt and Crowe, 1980) results were reported from experiments on isolated frog sartorius muscle subjected to controlled mechanical stretches of the ramp-and-hold type during tetanic contraction. The findings largely supported results carried out previously, on either single fibre preparations or bundles of fibres, with regard to such phenomena as the slip effect (Sugi, 1972) and excess tension after stretch (Edman *et al.*, 1976, 1978a, b).

In discussions of the possible mechanism by which these tension changes take place, it has been suggested that the cross bridges suffer elastic extensions which increase their contribution to the total tension but that attempted extension beyond an elastic limit causes mechanical breakage of the bridges (Van Atteveldt and Crowe, 1980; Sugi, 1972).

In order to test this idea, we have developed a model of the muscle which can be simulated on a digital computer by means of a "Continuous System Modelling Program" (CSMP). The model is based on the Huxley (1957) original theory of muscular contraction and further incorporates the actin-myosin overlap function to determine the total possible number of cross bridges according to the sarcomere length (Gordon *et al.*, 1966), together with passive components such as series elasticity, viscosity and non-linear parallel elasticity.

The simulated tension changes are compared with the experimental results presented in the previous article (Van Atteveldt and Crowe, 1980) and results of experiments on skeletal muscle presented by other authors (Edman *et al.*, 1976; Edman *et al.*, 1978a, b; Rack and Westbury, 1974; Sugi, 1972).

The reader is referred to the preceding article for a detailed description of the experimental methods and definitions and calculation of the percentage excess tension (PET).

THE SIMULATION MODEL

A four-element system containing a series elastic element (SEE), a parallel elastic element (PEE), a dashpot (D) representing a passive element with viscosity V , and a contractile element (CE) was set up as shown in Fig. 1a. The basic equation for the total force F_{SE} in the system is given by

$$F_{SE} = F_D + F_{CE} + F_{PE} \quad (1)$$

where F_{SE} , F_D , F_{CE} and F_{PE} are the forces obtaining in the components SEE, D, CE and PEE, respectively.

The tension generated will depend upon the state and duration of activation of CE and variation in time of the total length L of the muscle. In the present study the sarcomere length L_0 , at which maximum active tension is attained according to the actin-myosin overlap relationship, is given unity value. All other lengths, changes in length, and rates of change of length are expressed as percentages of this standard length.

Forces, both experimentally recorded and simulated, are expressed in newtons.

In our simulation we assume that the force in the dashpot D is linear with respect to \dot{y} . This is in keeping with experimental results (Alexander and Johnson, 1965; Buchthal and Kaiser, 1951). In any case, from our own experiments (Van Atteveldt and Crowe, 1980) it was seen that the tension changes due to the passive viscosity of the system were rather small compared to the total forces involved when active muscle was studied, so that possible non-linearities were of no consequence.

* Received for publication 22 May 1979.

† To whom proofs should be sent.

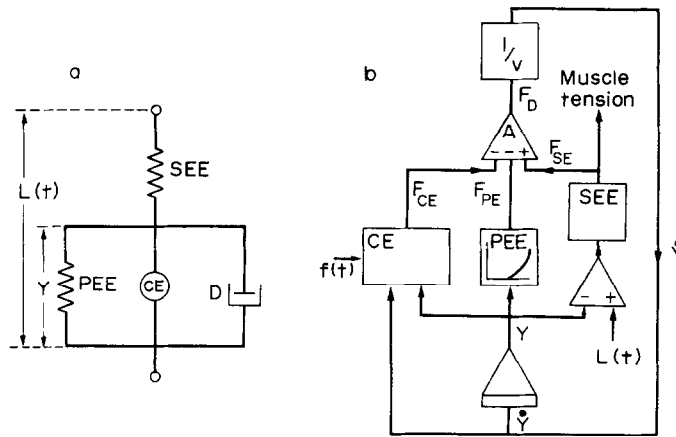


Fig. 1. (a) Schematic representation of muscle model. (b) Simplified analogue circuit of model.

The F_{SE} was taken to be proportional to the extension of the SEE, i.e. the parameter for the series elasticity (SE) was given a constant value in the simulations. The experimental results of Jewell and Wilkie (1958) indicate that this is a reasonable assumption.

Further details of the CE are given below but we are now in a position to set up the basic simulation circuit. This is given in Fig. 1b. The adder A represents equation (1) above. The inputs to the system are the time-varying length changes $L(t)$ and the muscle stimulation function $f(t)$. The simulation was done by means of a CSMP. Since the PEE is certainly non-linear, a function generator block is used for the simulation of F_{PE} .

Simulation of the CE

The model of the CE is in some ways similar to that put forward by Dijkstra *et al.* (1973). We assign the cross bridges into four bins according to their lengths (Fig. 2). Bin No. 1 has the shortest bridges and bin No. 4 the longest. The total numbers of bridges in each bin are denoted n_i ($i = 1-4$). All bridges within a particular bin exert the same tension E_i .

As a result of the sliding filament theory, exchange of bridges from one bin to another is possible when the actin moves with respect to the myosin during lengthening or shortening of the sarcomere. Further, it is assumed that a cross bridge is mechanically (as

opposed to biochemically) broken if its length is so great that it falls outside bin 4, or so small that it falls outside bin 1. This means that in our model no negative tension is exerted by the bridges and for the longer bridges, an elastic limit exists. Bridges can thus be broken by purely mechanical forces as well as by biochemical activity. Another assumption in our model is that cross bridges can only be made with an initial length such that they belong in bin 2 and immediately have the tension appropriate to that bin. In the other bins, the cross bridges can be broken and not made according to the equation

$$\frac{dn_i}{dt} = B_i - n_i g_i \quad (2)$$

$$i = 1, 3, 4$$

where g_i is the rate of breakdown through biochemical activity, and B_i is the function which gives the net rate of gain or loss to a bin from its neighbours through movement of the actin along the myosin. B_i thus depends upon the rate and direction of movement and the contents of the neighbouring bins.

The equation for the make and break of the bridges in bin 2 is

$$\frac{dn_2}{dt} = (N - n_2) \cdot [f(t) - n_2 g_2 + B_2] \quad (3)$$

where g_2 and B_2 have the same meanings as corresponding quantities in equation (2), $f(t)$ the stimulation function is the reaction rate for making the cross bridges and N is the maximum possible number of cross bridges in bin 2.

The function N was generated in the CSMP by a function generator block. Its values were determined on the basis of the relation between the total muscle tension and the amount of actin-myosin overlap. N was given a maximum value of unity for the most favourable overlap length and appropriate fractional values for other lengths.

Generation of the functions B_i was performed by first of all determining the values of $n_i |\dot{y}| a$, (where a is a constant and \dot{y} the rate of sarcomere length changes) and then directing them to the neighbouring higher or lower length bin according to whether the sarcomere

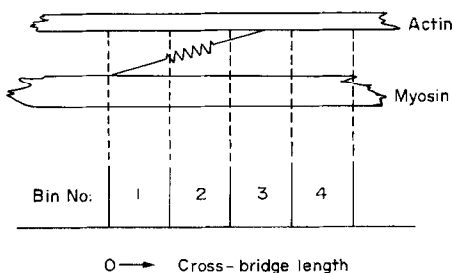


Fig. 2. Section of actin and myosin filament indicating how cross bridge length is assigned to one of four bins.

was being stretched or shortened. This was achieved in the simulation by means of relay blocks.

The value of F_{CE} is the sum of the tension contributions for the four bins

$$F_{CE} = \sum_{i=1}^4 n_i E_i \quad (4)$$

where E_i are constants and denote the contributions to the tension of the individual cross bridges in a particular bin.

Inputs to the model

The input $L(t)$ (Fig. 1) represents the initial length and superimposed stretch pattern. For the purposes of the present simulations only length changes of the ramp-and-hold type were used.

A special function block produced unit step pulses of predetermined onset and duration. These could be shaped by means of integrator and limiter blocks to adjust the speed and height of the ramp stretch.

The stimulation function $f(t)$ was simulated so that, at the onset of stimulation at t_0 , f rose exponentially to its maximum value f_{\max} according to the relation

$$f(t) = f_{\max} \{1 - \exp[-C_1(t - t_0)]\} \quad (5)$$

where C_1 is a constant. At the end of stimulation t_e , $f(t)$ decays exponentially to zero according to the relation

$$f(t) = f(t_e) \exp[-C_2(t - t_e)] \quad (6)$$

where C_2 is a constant.

The model could be programmed to produce single twitches, double twitches or fused tetani.

PARAMETER VALUES

We did not attempt to find parameter values which gave an exact simulation of the experimental situation seen when a muscle was stimulated and stretched. Had we done this values would have to be changed for each muscle since it was not possible, during the one experiment, to do all the different tests that were described below. Even more difficult would be an exact simulation of results of other authors since less experimental data are available to enable a fit to be made.

We decided, therefore, to use a basic set of simulation parameters from which we tried to obtain at least good qualitative representation of all the different experimental data, despite the fact that these resulted from different preparations. We deliberately chose passive elastic values to give a weak contribution to the total tension in keeping with experiments on single fibre or fibre bundle preparations. The functions $f(t)$ and g were chosen so that the tension rose fairly rapidly at the beginning of stimulation. This was done to economise on computer time.

The basic set of parameter values, so chosen that the time is measured in seconds, force in newtons, and lengths in terms of L_0 , are as follows:

$$\begin{aligned} a &= 266 \\ f_{\max} &= 30 \\ g &= 20 \\ E_i &= 0.4, 1, 2, 2.5 \\ &\quad (\text{for } i=1, 2, 3, 4 \text{ respectively}) \\ C_1 &= 10 \\ C_2 &= 20 \\ SE &= 60 \\ \frac{1}{V} &= 35 \end{aligned}$$

y	0	0.2	0.4	0.6	0.8	1.0	1.2	1.4	1.6	1.8	2.0
F_{PE}	0	0	0	0	0	0	0	0.05	0.2	0.5	0.8
actin-myosin overlap	0	0	0	0.4	0.8	1.0	1.0	0.6	0.3	0	0

RESULTS

Simulation of single twitches

Several authors (Bawa *et al.*, 1976; Carlson and Wilkie, 1974) have reported that, for a muscle at optimum length, changing the SE produces changes in the height and contraction time of a single twitch. The smaller the value of SE, the more slowly does the tension rise and the smaller is the peak value. This is simulated in Fig. 3 for a range of SE values. It is seen that the simulations are in qualitative agreement with the reported experiments (Bawa *et al.*, 1976) (Fig. 2, Ref. 3).

During the build-up of tension the SEE extends and thus the sarcomere shortens, since the isometric situation is being simulated. This shifts bridges from bin 2 where they are made, into the lower length bin 1 where they exert less tension. After the peak tension is reached the SEE shortens and those bridges remaining in bin 1 tend to be pulled out and exert higher tension before being broken. The number of bridges that enter and leave bin 1 in this way depends upon the extensibility of the SEE and determines the height and duration of the twitch. For a virtually non-extensible SEE all the bridges remain in bin 2. There is thus no reduction in tension by bridges being pulled into bin 1 and no delay in build-up of tension as a result.

Simulation of short-range stiffness

The short-range stiffness has been demonstrated (Rack and Westbury, 1974) in tetanized mammalian muscle, and Fig. 4 shows a record from our series of experiments on frog sartorius.

For moderate velocity stretches, the rate of increase in tension during the stretch is higher at the beginning than subsequently. Generally the steep rise in tension is seen during about the first 1% of stretch. Thereafter the slope is much more gentle and in some cases the tension may even remain steady during the stretch.

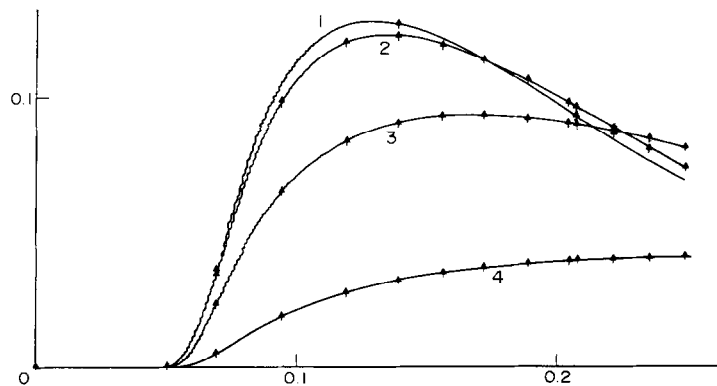


Fig. 3. Simulated single twitches to show influence of SE on duration and height of twitch. Values of SE were 1000, 100, 10 and 1 for curves 1–4 respectively. Vertical scale in newtons. Horizontal scale in seconds.

The simulation of short range stiffness is shown in Fig. 5. The initial rise in tension is produced by bridges being pulled out of bin 2 into bins 3 and 4 where they exert extra tension. The initial rate of gain by these bins exceeds the rate of loss. If the constant velocity stretch is continued the contents of the bins gradually tend to equilibrium levels where the net gain or loss due to biochemical activity is counterbalanced by the net gain or loss to neighbouring bins due to the actin–myosin movement.

From our simulation studies it appears that the short-range stiffness depends upon the SE. If this is increased, the rise in tension during the stretch, and

thus the short range stiffness, is increased. Reducing the SE has the opposite effect. For the larger SE values a proportionately greater stretch of the sarcomere is produced by a given muscle stretch. This increases the rate of actin–myosin movement and thus the rate at which cross bridges are pulled into the higher length bins. This makes for a sharp rise in tension and earlier attainment of steady values of the bin contents.

Simulation of the slip effect

It has been experimentally observed that, if the amount or speed of stretch are sufficiently large, the tension may reach a maximum value before the end of the ramp stretch (Van Attevelde and Crowe, 1980; Sugi, 1972). This is known as the slip effect. The conditions of stretch necessary to produce the effect seem to vary from muscle to muscle. In our experiments (Fig. 4b) stretches of 3.5% at $14.4\% \text{ s}^{-1}$ were sufficient to show the effect whereas Sugi (1972), using dissected semitendinosus bundles of fibres, found that the effect begins with stretch speeds of $2 \times 10^{3\%} \text{ s}^{-1}$ for a 5% stretch. Clearly, certain as yet uninvestigated factors play a role in the effect. Further Sugi (1972) has shown that a very rapid stretch produces first a peak tension and then a very rapid drop to below the isometric pre-stretch tension. At the beginning of the hold phase the tension then has to rise to attain the steady level. It is interesting that Sugi noticed that, during the hold phase, a secondary peak in the tension is reached before the final isometric level is reached (Fig. 6). This is also seen in the simulations (Figs. 7 and 8).

In those cases where the velocity of stretch is such that the slip effect just begins to show (Fig. 7), it is seen that the simulated stretches show good agreement with experiment (Fig. 4b). In each case a double peak is seen.

As can be seen from Fig. 7, the simulation of the slip effect arises from rather complicated patterns of the contents of bins 2, 3 and 4. The speed of stretch is such that no steady level is reached during the period of the stretch.

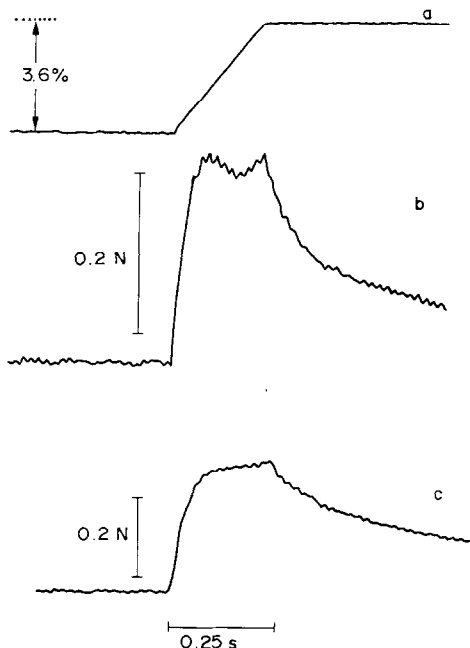


Fig. 4. Experimental records of stretch during tetanic contraction of frog sartorius muscles (a) length change ramp and hold record (b) muscle which just shows slip effect during stretch and (c) different muscle subjected to same stretch where slip effect does not appear but the short range stiffness during first part of stretch is clearly seen.

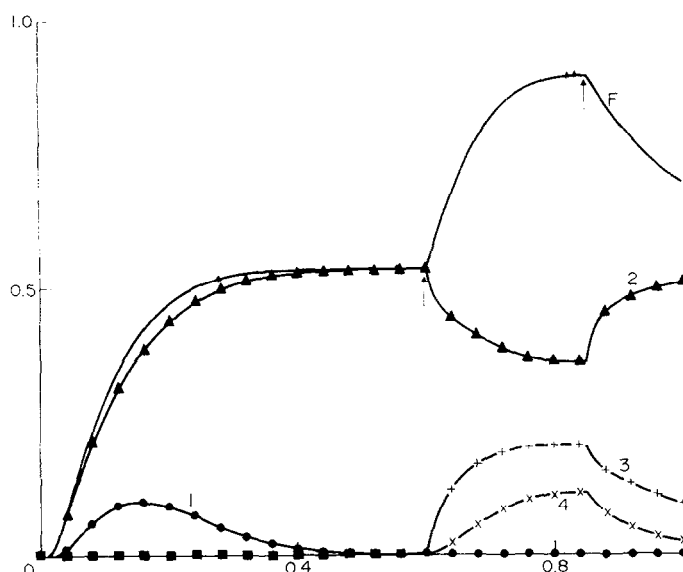


Fig. 5. Simulation of short range stiffness curve F , together with the contents of the bins curves 1-4 during tetanic stimulation and mechanical stretch. The vertical scale for the force F is in newtons and for the bin contents as a fraction of maximum total number of cross bridges. Horizontal scale in seconds. Vertical arrows indicate duration of ramp part of the stretch. Tetanic stimulation begins at time 0. See text and Fig. 2 for explanation of assignment of cross bridges to bins.

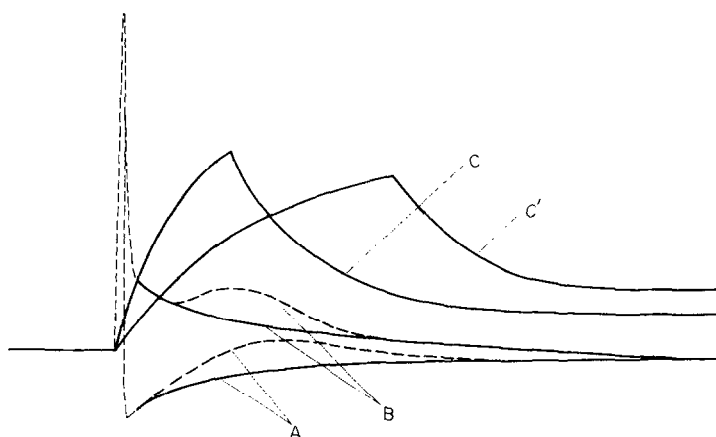


Fig. 6. Diagram showing experimentally obtained tension changes during and after stretches of various constant velocities applied to tetanically contracting frog semitendinosus fibre bundles. A, rapid stretch ($10-100 \text{ lengths s}^{-1}$) B, rapid stretch ($20-50 \text{ lengths s}^{-1}$). The early tension changes are indicated by thin interrupted lines on an expanded time scale. Thick interrupted lines represent the delayed transient rise of tension observed occasionally, C and C', moderate-velocity stretches (less than $10 \text{ lengths s}^{-1}$). Note the appearance of the hump in A and B prior to the tension assuming its final steady value. Figure reproduced with permission from H. Sugi, 1972.

For the faster stretches, we compare our simulations with the experimental results of Sugi reproduced here in Fig. 6. Our simulations show a peak tension before the end of the stretch. This is produced by an unloading of bin 2 into bins 3 and 4. If the stretch continues bins 3 and 4 are themselves unloaded and the tension begins to drop. The amount of fall in tension then depends upon the duration of the stretch. It is thus possible to simulate a fall in tension below the

isometric level. During the restoration of the tension after the stretch, the pattern is very similar to that seen in Sugi's experiments. In particular, it is noticed that the tension initially rises above its final steady value.

Simulation of excess tension

When a muscle is stretched during a tetanic stimulation, the tension at the new length is greater than if the muscle had been stretched to the new length before

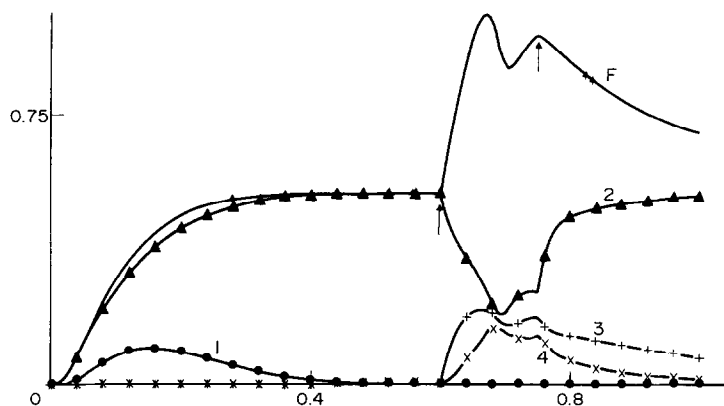


Fig. 7. Simulation of slip effect F to show how double peak effect arises from contents of bins 1–4 during stretch. Total tension record to be compared with experimental record of Fig. 4(b). Same notation and terminology as for Fig. 5.

stimulation had begun. This difference in tension, measured in each case at equal times from the onset of stimulation, is known as the excess tension. It is better expressed as a percentage of the tetanic tension. This we call the percentage excess tension (PET). Its precise definition and methods of calculation are given in the preceding article (Van Attevelde and Crowe, 1980). If a particular stretch, that did not lead to a slip effect, was applied to the muscle while it was held at different begin lengths, a length dependence on the magnitude and rate of decay of the PET was observed. At the shorter muscle lengths i.e. below that for optimal

active tension, the initial or peak PET (i.e. the PET at the end of the ramp phase of the stretch) had constant values. At muscle lengths above the optimum the initial PET increased with length. Furthermore, it was seen that the rate of decay of PET was faster for the shorter muscle lengths than for the longer lengths.

The PET values have been calculated from simulated stretches applied over a range of total muscle lengths. The results are plotted in Fig. 9 together with the corresponding tension-length curves for isometric tensions. These simulations should be compared with the experimentally derived results given in Fig. 6 of the

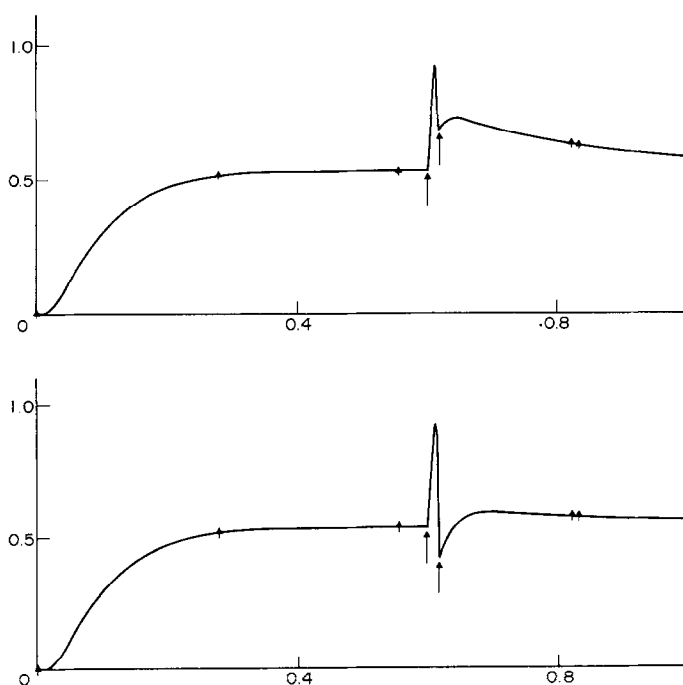


Fig. 8. Simulations of force during faster stretches to show slip effect. Records to be compared with experimental records of Figs. 6(a) and (b). Same notation as for simulations in previous figures.

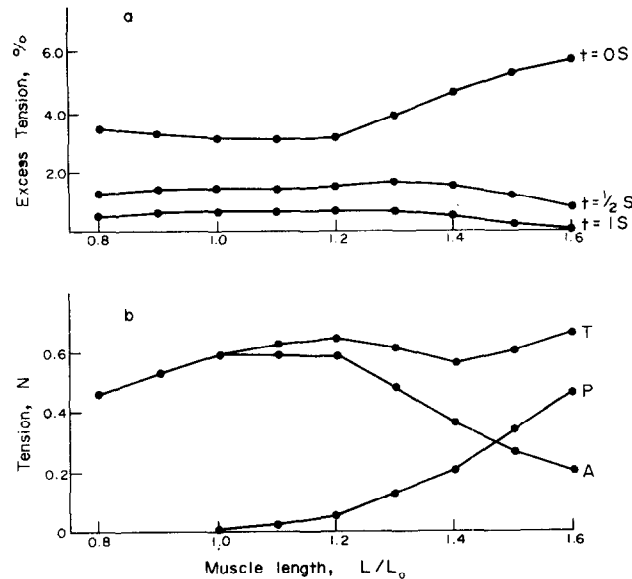


Fig. 9. (a) Measurement of PET from simulations of stretches at different muscle lengths. Note how the peak PET (i.e. at 0 s) increases for lengths greater than that needed for maximal isometric contraction, yet the rate of decay, as seen from the PET values at $\frac{1}{2}$ and 1 s, increases at these muscle lengths. (b) Corresponding simulated length/tension curves showing total tension T , passive tension P and active tension A obtained from the simulations used to obtain the curves in (a). See preceding article for method of calculation of PET.

preceding article (Van Attevelde and Crowe, 1980). As already mentioned, the values of the elasticity in the simulations were deliberately chosen to be lower than those for experiments on whole muscle, and thus the contribution of the passive tension to the total tension in the simulations is smaller (Fig. 9b).

In Fig. 9(a) it is seen that the simulated initial PET values ($t = 0$ s) follow a similar pattern with respect to muscle length as do the experimental values. On the other hand our simulations predict a more rapid decay of PET at longer muscle lengths than for shorter lengths. This is contrary to the experimental findings and in this respect the model is deficient.

DISCUSSION

As a basis for the simulations we relied upon the original theoretical model of Huxley (1957) but certain simplifications were introduced. In the first place the lengths of the cross bridges were restricted to four discrete groups or bins.

The choice of four bins was not entirely arbitrary. Apart from the bin in which the bridges were made, it was felt that the bridges should, by reduction of the sarcomere length, be allowed to shorten and exert less tension. Further, it was found that by having more than two bins into which the bridges could be extended, no substantial improvement in the simulations was made, but just one bin certainly gave inferior simulations. Thus four bins in total were chosen.

The f and g functions for the make and break of the cross bridges were also simplified. The function g was given the same value irrespective of cross bridge length

and the function f was such that cross bridges of only a particular length could be created. It is possible that the function f could also depend upon the speed of relative movement of the actin and myosin, but the model was not modified to include this idea. Also, no account is taken of possible changes in f due to changes in calcium binding properties at different sarcomere lengths.

Further, we have not incorporated in the model the now rather widely-accepted idea that bridges can exert negative tension. This omission is not to be interpreted as a disagreement with the idea but was made because it was intended to test the model in situations where the stimulated muscle was mechanically stretched. In such situations bridges in negative tension would hardly contribute to the total force. It has to be admitted, however, that bridges in negative tension could play a role in purely isometric contractions which produce shortening in the sarcomere as it pulls against a weak SEE.

According to modern views on cross bridge structure (Huxley, 1974) the tension is generated because the bridges consist of an elastic element joined to a hinged element. Upon attachment, the hinged element rotates and generates a tension by extending the elastic element. By restricting the making of the cross bridges to just one bin so that they are immediately assigned a tension, we have effectively incorporated the hinged bridge system in the model.

In spite of all the simplifications, a large number of parameters still has to be chosen. But nonetheless, many recently reported phenomena observed in isometric twitches or when contracting muscle is stretched

are qualitatively rather well simulated. We are, of course, aware that the model is rather selectively tested. No attempt has been made to simulate, for example, features observed when contracting muscle is allowed to shorten. This we felt unnecessary because our model is essentially an adaptation of the Huxley model which, in its original or modified form, is quite adequate to simulate such features.

An aspect of the simulations which does not bear satisfactory resemblance to experimental findings concerns the dependance of the rate of decay of PET to the total muscle length. We did not find from our simulations a slower decay for the longer muscle lengths. This is contrary to what is observed in whole muscle (Van Atteveldt and Crowe, 1980) where passive forces contribute to the stretch tension for lengths greater than L_0 , and in single fibre preparations (Edman *et al.*, 1978) where the contribution of passive forces is relatively small. It would appear then that the length dependance of the observed phenomena is not due to passive properties of the muscle. We suggested in our previous paper (Van Atteveldt and Crowe, 1980) that effects due to total muscle length might be due to non-uniform properties of cross bridges. Those attached to the ends of the myosin might have different stability properties due to configuration differences compared to the other cross bridges. We have not introduced such a modification in our simulation model. Better agreement between experiment and simulation could probably be obtained but only at the expense of a more complicated simulation and the necessity for extra parameter values.

Apart from this deficiency in the model it has nonetheless served to show that many of the more recently observed phenomena of muscle can be reasonably well explained if certain assumptions regarding the properties of the cross bridges are made, viz, that they are extensible and exert a tension related, not necessarily linearly, to their length; that they can be stretched to breaking point by physical forces; and that the tension changes seen during the movement of the actin and myosin depend upon the speed of this movement in relation to the rates of biochemical activity for the make and break of the bridges.

Acknowledgements – The authors are grateful to Professor H. Sugi and the Editorial Board to the *Journal of Physiology* for permission to use the material which is reproduced as Fig. 6 of this paper and to Prof. J. J. Denier van der Gon and other colleagues for their comments and criticism of the manuscript.

REFERENCES

- Alexander, R. S. and Johnson, P. D. (1965) Muscle stretch and theories of contraction, *Am. J. Physiol.* **208**, 412–416.
- Van Atteveldt, H. and Crowe, A. (1980) Active changes in frog skeletal muscle during and after mechanical extension, *J. Biomechanics*, **13**, 323–331.
- Bawa, P., Mannard, A. and Stein, R. B. (1976) Effects of elastic loads on contractions of cat muscles, *Biol. Cybernetics* **22**, 129–137.
- Buchthal, F. and Kaiser, E. (1951) The rheology of the cross-striated muscle fibre with special reference to isotonic conditions, *Dan. Biol. Med.* **21**, 318.
- Carlson, F. P. and Wilkie, D. R. (1974) *Muscle Physiology* (Edited by Prentice Hall), p. 41. Englewood Cliffs, New Jersey.
- Dijkstra, S., Denier van der Gon, J. J., Blangé, T., Karemaker, J. M. and Kramer, A. E. J. L. (1973) A simplified sliding-filament muscle model for simulation purposes, *Kybernetik* **12**, 94–101.
- Edman, K. A. P., Elzinga, G. and Noble, M. I. M. (1976) Force enhancement induced by stretch of contracting single isolated muscle fibres of the frog, *J. Physiol.* **258**, 95–96p.
- Edman, K. A. P., Elzinga, G. and Noble, M. I. M. (1978) Further characterization of the enhancement of force by stretch during activity in single muscle fibres of the frog, *J. Physiol.* **280**, 35–36p.
- Edman, K. A. P., Elzinga, G. and Noble, M. I. M. (1978) Enhancement of mechanical performance by stretch during tetanic contractions of vertebrate skeletal muscle fibres, *J. Physiol.* **281**, 139–155.
- Gordon, A. M., Huxley, A. F. and Julian, F. J. (1966) The variation in isometric tension with sarcomere length in vertebrate muscle fibres, *J. Physiol.* **184**, 170–192.
- Huxley, A. F. (1957) Muscle structure and theories of contraction, *Prog. Biophys. biophys. Chem.* **7**, 255–318.
- Huxley, A. F. (1974) Muscular contraction, *J. Physiol.* **243**, 1–43.
- Jewell, B. R. and Wilkie, D. R. (1958) An analysis of the mechanical component in frog's striated muscle, *J. Physiol.* **143**, 515–540.
- Rack, P. M. H. and Westbury, D. R. (1974) The short range stiffness of active mammalian muscle and its effect on mechanical properties, *J. Physiol.* **240**, 331–350.
- Sugi, H. (1972) Tension changes during and after stretch in frog muscle fibres, *J. Physiol.* **225**, 237–252.